Journal of the Arkansas Academy of Science

Volume 69 Article 12

2015

Wave Profile for Anti-force Waves with Maximum Possible Currents

M. Hemmati
Arkansas Tech University, mhemmati@atu.edu

R. Horn
Arkansas Tech University

W. P. Childs
Arkansas Tech University

A. K. Meredith
Arkansas Tech University

Wave Profile for Anti-force Waves with Maximum Possible Currents

M. Hemmati[1*], R. Horn[1], W.P. Childs[1] and A.K. Meredith[1]

[1]*Department of Physical Sciences, Arkansas Tech University, Russellville, Arkansas 72801, USA*

*Correspondence: mhemmati@atu.edu

Running Title: Wave Profile for Anti-force Waves with Maximum Possible Currents

Abstract

In the theoretical investigation of the electrical breakdown of a gas, we apply a one-dimensional, steady state, constant velocity, three component fluid model and consider the electrons to be the main element in propagation of the wave. The electron gas temperature, and therefore the electron gas partial pressure, is considered to be large enough to provide the driving force. The wave is considered to have a shock front, followed by a thin dynamical transition region. Our set of electron fluid-dynamical equations consists of the equations of conservation of mass, momentum, and energy, plus the Poisson's equation. The set of equations is referred to as the electron fluid dynamical equations; and a successful solution thereof must meet a set of acceptable physical conditions at the trailing edge of the wave.

For breakdown waves with a significant current behind the shock front, modifications must be made to the set of electron fluid dynamical equations, as well as the shock condition on electron temperature. Considering existence of current behind the shock front, we have derived the shock condition on electron temperature, and for a set of experimentally measured wave speeds, we have been able to find maximum current values for which solutions to our set of electron fluid dynamical equations become possible. We will present the wave profile for electric field, electron velocity, electron temperature, and electron number density within the dynamical transition region of the wave.

Introduction and Model

The electrical breakdown of a gas in the presence of a high electric field occurs by a wave propagating with speeds approaching the speed of light and a discontinuity at the wave front. The most common form of breakdown waves in nature is lightning strokes of varying classifications. The basic model consists of a volume of excess charge (electron gas) advancing into a neutral gas, partially ionizing the neutral gas. In anti-force waves (Lightning return strokes), the direction of the electric field force on the electrons causes an electron mobility motion in the opposite direction of the wave propagation. However, the electron gas temperature, and therefore the electron gas partial pressure, is large enough to provide the net force for propagation of the wave. Return strokes in lightning can consist of a wave for which a large current exists behind the shock front.

The basic set of equations which apply to electron gas alone, consists of the equations of conservation of mass, momentum and energy; and the Maxwell's equations reduces to the Poisson's equation alone. The wave front is considered to be a shock front, followed by a thin dynamical transition region, referred to as the sheath region of the wave. In the sheath region, the electric field and electron velocity are changing rapidly; however, the changes in the electron number density and temperature are not so rapid by comparison. The sheath region is followed by a relatively thicker region, referred to as the quasi-neutral region of the wave; where in this region the electric field is zero, and because of further ionization of heavy particles, the electron gas cools down to room temperature and the electrons slow down to speeds comparable to those of heavy particles.

For theoretical investigation of breakdown waves, we employ the set of equations developed by Fowler et al. (1984). Their set of equations which describe pro-force waves consists of the equations of conservation of mass, momentum, and energy coupled with the Poisson's equation. The set of equations respectively are

$$\frac{d(n\upsilon)}{dx} = n\beta, \tag{1}$$

$$\frac{d}{dx}[mn\nu(\upsilon - V) + nkT_e] = -enE - Kmn(\upsilon - V), \tag{2}$$

$$\frac{d}{dx}[mn\upsilon(\upsilon-V)^2+nkT_e(5\upsilon-2V)+2en\upsilon\Phi-\frac{5nkT_e}{mK}\frac{dT_e}{dx}]$$
$$=-3(\frac{m}{M})nkKT_e-(\frac{m}{M})Kmn(\upsilon-V)^2, \quad (3)$$

$$\frac{dE}{dx}=\frac{e}{\varepsilon_0}n(\frac{\nu}{V}-1). \quad (4)$$

Where ν, n, T_e, m and e represent electron velocity, number density, temperature, mass and charge respectively. $E_0, E, V, M, K, k, \beta, \phi, x$, represent electric field at the shock front, electric field within the sheath region of the wave, wave velocity, neutral particle mass, elastic collision frequency, Boltzmann's constant, ionization frequency, ionization potential of the gas and position within the sheath region of the wave respectively.

To be able to integrate the set of equations (1-4) through the sheath region of the wave, Fowler et al. (1984) reduced the set of equations to non-dimensional form. Fowler et al's (1984) set of non-dimensional variables are

$$\eta=\frac{E}{E_o}, \nu=(\frac{2e\phi}{\varepsilon_o E_o^2})n, \psi=\frac{\nu}{V}, \theta=\frac{T_e k}{2e\phi}, \xi=\frac{eE_o x}{mV^2},$$
$$\alpha=\frac{2e\phi}{mV^2}, \kappa=\frac{mV}{eE_o}K, \mu=\frac{\beta}{K}, \omega=\frac{2m}{M},$$

where $\eta, \nu, \psi, \theta, \mu$ and ξ represent the non-dimensional electric field, electron number density, electron velocity, electron gas temperature, ionization rate, and position within the sheath region of the wave, respectively; while α and κ represent wave parameters. Substituting the non-dimensional variables in equations (1-4), the set of equations become

$$\frac{d(\nu\psi)}{d\xi}=\kappa\mu\nu, \quad (5)$$

$$\frac{d}{d\xi}[\nu\psi(\psi-1)+\alpha\nu\theta]=-\nu\eta-\kappa\nu(\psi-1), \quad (6)$$

$$\frac{d}{d\xi}[\nu\psi(\psi-1)^2+\alpha\nu\theta(5\psi-2)+\alpha\nu\psi+\alpha\eta^2-$$
$$\frac{5\alpha^2\nu\theta}{\kappa}\frac{d\theta}{d\xi}]=-\omega\kappa\nu[3\alpha\theta+(\psi-1)^2], \quad (7)$$

$$\frac{d\eta}{d\xi}=\frac{\nu}{\alpha}(\psi-1). \quad (8)$$

In the case of theoretical investigation of anti-force waves, we employ the set of dimensionless variables developed by Hemmati (1999); in which all quantities including κ are positive, and the position within the sheath, ξ, is positive backward. Hemmati's (1999) set of dimensionless variables for anti-force waves, which have proven to be successful are

$$\eta=\frac{E}{E_o}, \nu=(\frac{2e\phi}{\varepsilon_o E_o^2})n, \psi=\frac{\nu}{V}, \theta=\frac{T_e k}{2e\phi}, \xi=-\frac{eE_o x}{mV^2},$$
$$\alpha=\frac{2e\phi}{mV^2}, \kappa=-\frac{mV}{eE_o}K, \mu=\frac{\beta}{K}, \omega=\frac{2m}{M}.$$

For anti-force waves (lightning return strokes) with a large current behind the wave front, in addition to the equation of conservation of energy and the Poisson's equation, the boundary condition on electron temperature at the shock front must be modified as well. For anti-force waves with a large current behind the wave front, we will use Hemmati et. al's (2011) modified set of non-dimensional equations.

$$\frac{d}{d\xi}[\nu\psi]=\kappa\mu\nu, \quad (9)$$

$$\frac{d}{d\xi}[\nu\psi(\psi-1)+\alpha\nu\theta]=\nu\eta-\kappa\nu(\psi-1), \quad (10)$$

$$\frac{d}{d\xi}[\nu\psi(\psi-1)^2+\alpha\nu\theta(5\psi-2)+\alpha\nu\psi-\frac{5\alpha^2\nu\theta}{\kappa}\frac{d\theta}{d\xi}$$
$$+\alpha\eta^2]=2\eta\kappa\iota\alpha-\omega\kappa\nu[3\alpha\theta+(\psi-1)^2], \quad (11)$$

$$\frac{d\eta}{d\xi}=\kappa\iota-\frac{\nu}{\alpha}(\psi-1). \quad (12)$$

Where, with I_1 representing the current behind the wave front,

$$\iota=\frac{I_1}{\varepsilon_0 KE_0}, \quad (13)$$

is the dimensionless current behind the wave front. We will use Hemmati et al's (2011) modified boundary condition on electron temperature at the shock front as well

$$\theta_1=\frac{\psi_1(1-\psi_1)}{\alpha}-\frac{\kappa\iota}{\nu_1}. \quad (14)$$

Where, θ_1, ν_1 and ψ_1, represent the electron temperature, number density and velocity values at the shock front.

Results and Discussion

Examining characteristics of the initial stage in lightning initiated from tall objects and in rocket-triggered lightning, Miki et al. (2005) report mean peak current of 8.8 kA for return stroke current pulses; however, they also reported lightning currents as high as 150 kA measured at the Fukui thermal plant station in Japan. In a study of propagation characteristics of lightning leaders and return strokes, Olsen et al. (2006) report rocket-triggered lightning currents typically in the range of 1 kA; however, triggered or natural lightning subsequent stroke currents are in the range of 10-15 kA. In a review of characteristics of lightning discharges that transport either positive charge or both negative and positive charges to ground, Rakov (2000) reported positive return stroke (positive flashes) currents in excess of 10 kA, an order of magnitude larger than for negative flashes. Rakov (2000) also reported direct current measurements of three positive lightning discharges in Japan with very large peaks of 340, 320, and 280 kA of initial pulses. In his review article, Rakov (2000) reported return stroke speeds in the range of $0.3x10^8 m/s$ to $1.7x10^8 m/s$. However, imaging of upward positive leaders in two artificially-initiated lightning flashes, Yoshida et al. (2010) report average steady current of 2 kA, and a peak current value of 18 kA; where their reported speed was on the order of $10^6 m/s$.

Determining the ratio of the elastic collision frequency, K (McDaniel 1964), to the electron gas pressure, P, gives $K/P = 3x10^8$ for helium and $K/P = 4.8x10^7$ for nitrogen at 273 K. At a temperature of 10^5 K, this will be $2.4x10^9$ for helium and $9x10^9$ for nitrogen and applied fields are usually of the order $10^5 V/m$. Considering that E_0, K, β in our formulas are scaled with P (the electron gas pressure) and using the values of $I_1, \varepsilon_0, E_0, K$ one can estimate the value of ι, which is of order one.

We use a numerical trial-and-error method to integrate equations 9 - 12 through the sheath region of the wave. For a given wave speed, α, a set of values for wave constant, κ, electron velocity ψ_1 and electron density, ν_1 at the wave front are chosen. The values of κ, ψ_1 and ν_1 are repeatedly changed in integrating equations 9 -12 through the sheath region of the wave, until the process leads to a satisfactory conclusion meeting the expected physical conditions at the end of the sheath region of the wave.

$$\left[\eta_2 \to 0, \quad \psi_2 \to 1, \quad \left(\frac{d\eta}{d\xi}\right)_2 \to 0, \quad \left(\frac{d\psi}{d\xi}\right)_2 \to 0\right]. \quad [15]$$

For α = 0.001, 0.01, 0.1 and 1, we have been able to integrate the set of electron fluid dynamical equations (equations 9-12) for maximum non-dimensional current, ι, values of 7, 5, 1 and 0.5 respectively, for which solutions to the set of equations became possible and met the expected physical conditions at the trailing edge of the wave. α =0.001 represents a fast wave speed of $0.937x10^8 m/s$ and α = 1 represents a very low wave speed of $0.3x10^7 m/s$ for lightning return strokes. In a review of available experimental data on return-stroke speed for both negative and positive lightning, minimum return-stroke speed reported by Rakov (2007) was $2x10^7 m/s$.

The successful solutions for the indicated speeds, α, and dimensionless currents, ι, required the following boundary values

$$\alpha = 0.001, \iota = 7, \kappa = 0.144, \psi_1 = 0.4721, \nu_1 = 0.2161$$
$$\alpha = 0.01, \iota = 5, \kappa = 1.3, \psi_1 = 0.7, \nu_1 = 0.7696$$
$$\alpha = 0.1, \iota = 1, \kappa = 0.44, \psi_1 = 0.832, \nu_1 = 0.71$$
$$\alpha = 1, \iota = 0.5, \kappa = 0.1338, \psi_1 = 0.5502, \nu_1 = 0.4882$$

Figure 1 represents dimensionless electric field, η, as a function of dimensionless electron velocity, ψ, within the sheath region of the wave. For all dimensionless wave speed and current values, our solutions meet the expected conditions at the end of the sheath region of the wave. Upon close inspection of the curve with α = 0.001 and ί = 7, it seems that the electric field value at the shock front starts at 3; although that is not the case. During integration of the set of electron fluid dynamical equations through the sheath region, particularly for slower wave speeds and larger current values, the sheath thickness become relatively large, making the number of data points also very large. To keep it uniform for all wave speeds and current values, only one out of every ten data points is print. Therefore, the first point indicated in the curve for α = 0.001 and ί = 7, is actually the tenth data point. However, as was indicated, we have been able to solve the set of equations for lower speeds than those observed experimentally. Also, for large current values and slow wave speeds, integration of the set of electron fluid dynamical equations through the sheath region of the wave becomes very time consuming and difficult.

Wave Profile for Anti-force Waves with Maximum Possible Currents

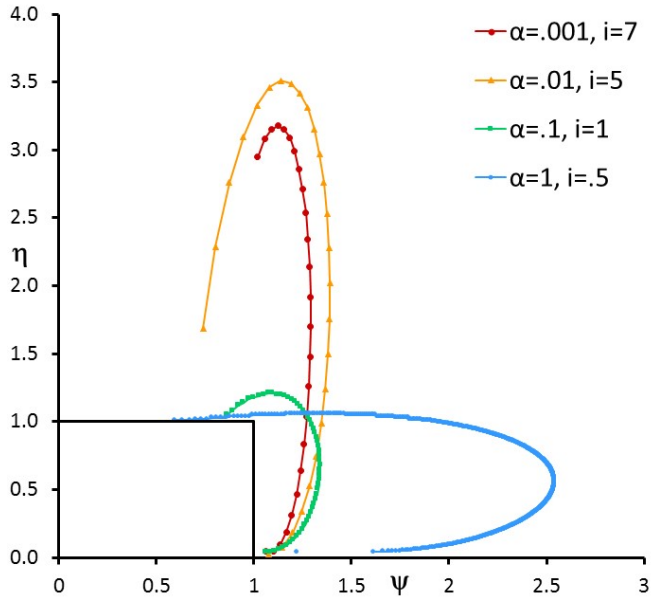

Figure 1: Electric field, η, as a function of electron velocity, ψ, within the sheath region of anti-force current bearing waves for wave speed values of α = 0.001, 0.01, 0.1, 1, and maximum dimensionless current values of 7, 5, 1, and 0.5, for which solutions to the set of electron fluid dynamical equations became possible.

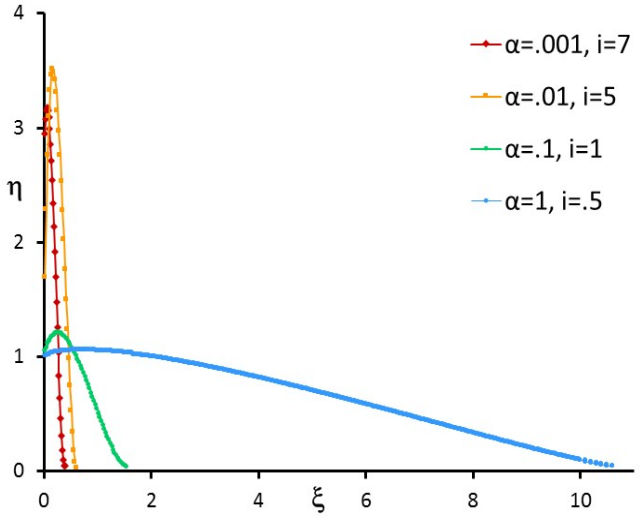

Figure 2: Electric field, η, as a function of position, ξ, within the sheath region of anti-force current bearing waves for wave speed values of α = 0.001, 0.01, 0.1, 1, and maximum dimensionless current values of 7, 5, 1, and 0.5, for which solutions to the set of electron fluid dynamical equations became possible.

Figure 2 represents dimensionless electric field, η, as a function of dimensionless position, ξ, within the sheath region of the wave for anti-force current bearing waves. The curve for α = 1 and í = 5, shows that the sheath thickness is much larger than that for α = 0.001 and í = 7.

Figure 3 represents the dimensionless electron velocity, ψ, as a function of dimensionless position, ξ, within the sheath region, for anti-force current bearing waves. For all α values, solutions of the set of electron fluid dynamical equations met the expected boundary conditions at the trailing edge of the wave; nevertheless, for α = 1 and í = 0.5, in integration of the set of equations through the sheath region of the wave, the best value we could find ψ_2 was 1.22.

Figure 4 represents electron gas temperature, θ, as a function of position, ξ, within the sheath region of anti-force current bearing waves. As α decreases and wave speed increases, the electron gas temperature becomes very large. For α = 0.1, meaning wave speed of 9.37×10^6 m/s, our dimensionless electron temperature of approximately 1, corresponds to a temperature of 5.8×10^5 K. For the wave speed of 9.37×10^6 m/s, our electron temperature value within the sheath region of the wave, agrees well with the electron temperature reported by Sanmann (1975) for an anti-force wave with a similar wave speed.

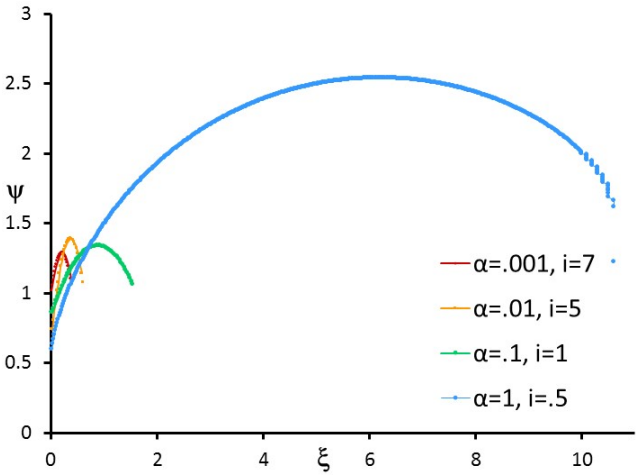

Figure 3: Electron velocity, ψ, as a function of position, ξ, within the sheath region of anti-force current bearing waves for wave speed values of α = 0.001, 0.01, 0.1, 1, and maximum dimensionless current values of 7, 5, 1, and 0.5, for which solutions to the set of electron fluid dynamical equations became possible.

Figure 5 represents dimensionless electron number density, ν, as a function of position within the sheath region of anti-force current bearing waves. For α = 0.1 and wave speed of 9.37×10^6 m/s, our average dimensionless electron number density of 0.6, corresponds with electron number of 7.7×10^{15} electrons/m^3. Again, for a wave speed of 9.37×10^6 m/s, our electron number density value compares well with the electron number density for an anti-force wave of

similar wave speed reported by Sanmann (1975).

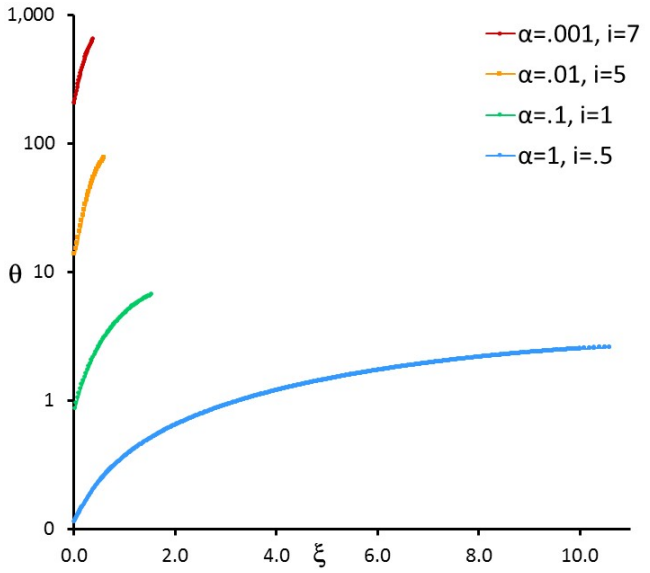

Figure 4: Electron temperature, θ, as a function of position, ξ, within the sheath region of anti-force current bearing waves for wave speed values of α = 0.001, 0.01, 0.1, 1, and maximum dimensionless current values of 7, 5, 1, and 0.5, for which solutions to the set of electron fluid dynamical equations became possible.

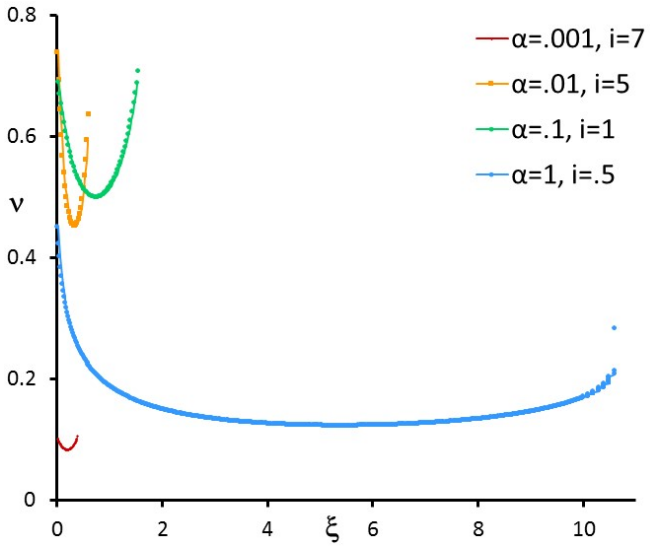

Figure 5: Electron number density, ν, as a function of position, ξ, within the sheath region of anti-force current bearing waves for wave speed values of α = 0.001, 0.01, 0.1, 1, and maximum dimensionless current values of 7, 5, 1, and 0.5, for which solutions to the set of electron fluid dynamical equations became possible.

Conclusions

For current bearing anti-force waves, we have been able to solve our set of electron fluid dynamical equations for the range of current values reported by experimentalists. In fact, we have been able to integrate the set of equations for larger current values, which have been reported by a few experimentalists as well; indicating that in lightning return strokes, such large currents may exist. Also, we have been able to integrate our set of electron fluid dynamical equations for much lower speeds than those reported experimentally, implying that return strokes with lower wave speeds should be detected as well. For anti-force current bearing waves, as wave speed increases, the current values for which solutions for the set of electron fluid dynamical equations become possible increases as well. As the wave speed decreases and the current value increases, integration of the set of electron fluid dynamical equations through the sheath region of the wave becomes time consuming and difficult.

Acknowledgement

The authors would like to express gratitude for the financial support provided by the Arkansas Space Grant Consortium.

Literature Cited

Fowler RG, **M Hemmati**, **RP Scott**, and **S Parsenajadh**. 1984. Electric breakdown waves: Exact numerical solutions. Part I. The Physics of Fluids 27(6):1521-1526.

Hemmati M. 1999. Electron shock waves: speed range for anti-force waves. Proceedings of the 22nd International Symposium on Shock Waves; 1999 July 18-23; Imperial College, London, UK. Pp. 2:995-1000.

Hemmati M, **WP Childs**, **H Shojaei** and **DC Waters**. 2011. Antiforce current bearing waves. Proceedings of the 28th International Symposium on Shock Waves (ISSW28), July 2011, England.

McDaniel EW. 1964. Collision phenomena in ionized gases. Wiley, New York

Miki M, **VA Rakov**, **T Shindo**, **G Diendorfer**, **M Mair**, **F Heidler**, **W Zischank**, **MA Uman**, **R Thottappillil** and **D Wang**. 2005. Initial stage in lightning initiated from tall objects and in rocket-triggered lightning. Journal of Geophysical Research. 110: D02109.

Olsen III RC, **VA Rakov**, **DM Jordan**, **J Jerauld**, **MA Uman**, and **KJ Rambo**. 2006. Leader/return-stroke-like processes in the initial stage of rokect-triggered lightning. Journal of Geophysical Research 111:D13202.

Rakov VA. 2000. Positive and bipolar lightning discharges: a review. Proc. 25th Int. Conference on Lightning Protection. 103-108.

Rakov VA. 2007. Lightning return stroke speed. Journal of Lightning Research. 1:80-89.

Sanmann E and **RG Fowler**. 1975. Structure of Electron Fluid Dynamical Plane Waves: Anti-force Waves. The Physics of Fluids, 18(11): 1433-8.

Yoshida S, **CJ Biagi**, **VA Rakov**, **JD Hill**, **MV Stapleton**, **DM Jordan**, **MA Uman**, **T Morimoto**, **T Ushio** and **ZI Kawasaki**. 2010. Three-dimensional imaging of upward positive leaders in triggered lightning using VHF broadband digital interferometers. Geophysical Research Letters. 37:L05805.